

Crash Simulation of Mechanical Joints with Automatically Determined Model Parameters based on Test Results and Prediction Algorithms

S. Sommer¹, P. Rochel¹, M. Guenther², D. Herfert²,
G. Meschut³; P. Giese³

¹Fraunhofer IWM, Germany; ²Society for the Advancement of Applied Computer Science GFaI, Germany;

³Laboratory for material and joining technology LWF, Germany

Abstract

*The increasing usage of innovative light weight concepts in automobile production leads to the application of different mechanical joining techniques like self-pierce riveting- semi tubular (SPR-ST) and -solid (SPR-S), flow drilling screwing (FDS) and high speed bolt joining (HSB) for multi-material constructions. These mechanical joints are used at positions of car bodies which show high stresses under impact loading. For the prediction of the load-bearing capacity, the failure behavior and the energy absorption in crash simulations complete and reliable models are needed. Therefore experimental results on single joint specimens and simulation of these specimen tests are necessary to determine the model parameters. If this had to be done for all existing sheet metal combinations of all mechanical joints in a body-in-white it would result in a very time and cost intensive process. The aim of the research project "CraSiFue"[1] was to reduce these efforts by developing a forecast algorithm and implementing it in a software. The developed software JoiningLab predicts the joint properties and model parameters of the *CONSTRAINED_INTERPOLATION_SPOTWELD (Model 2, "SPR4") [2], [3] in LS-DYNA[®] for untested i.e. unknown mechanical joints. This results in saving real tests and accelerates the crash safety investigations especially in the concept phase of construction, where materials, sheet thicknesses and joints are not definitely specified yet.*

Introduction

The experimental tests on single joint specimens for the above mentioned mechanical joining techniques have been performed by the Laboratory for Materials and Joining Technology (LWF), University of Paderborn, Germany. Therefore the LWF-KS-2 testing concept and LWF-KS-2-peel specimens were used to determine the load-bearing capacity and the failure behavior. The tested joints vary in material combination, sheet thickness and mechanical joining technique to delimit the boundaries of still joinable combinations. These tests combined with results of former IGF projects constituted the database for the prediction algorithm of the software JoiningLab, which was developed and implemented by Society for the Advancement of Applied Computer Science (GFaI), Berlin, Germany. It is now possible to predict joint properties i.e. characteristic values like load-bearing capacities under tension or shear loading and special points of the force displacement curve of unknown joints. The Fraunhofer Institute for Mechanics of Materials (IWM) Freiburg, Germany, has developed transformation rules to calculate the parameters of the *CONSTRAINED_INTERPOLATION_SPOTWELD (Model 2, "SPR4") out of given force vs. displacement curves automatically. Because sheet metal deformations are still included in the measured force vs. displacement curves of single joint specimen tests some assumptions are necessary here. These transformation rules are also implemented in the software JoiningLab and can be used for measured i.e. well known joint properties as well as for predicted properties of not yet tested joints. The automatically determined model parameters are written in the input card format of LS-DYNA. For validation purpose of the prediction algorithm as well as for the automatically calculated model parameters mechanical joints which are not included in the prediction have been tested and simulated.

Characterization of mechanical joints as a database for prediction and crash modelling

The experimental tests on single joint specimens for the mechanical joining techniques have been performed by the Laboratory for Materials and Joining Technology (LWF), University of Paderborn, Germany. Therefore the LWF-KS-2 testing concept and LWF-KS-2-peel specimens were used to determine the load-bearing capacity and the failure behavior of different mechanical joints and material combinations including different sheet thicknesses t . The characteristic force vs. displacement curves for a SPR-ST joint under impact loading are shown in Figure 1. For each load angle a test series of five repeated attempts are conducted. During the tests under a high loading velocity of 1 m/s an interaction of dynamic effects i.e. oscillations in the force measurement signals occurs, that shows varying degree depending on the load angle. However, the influence on the determined maximum forces can be considered as negligible.

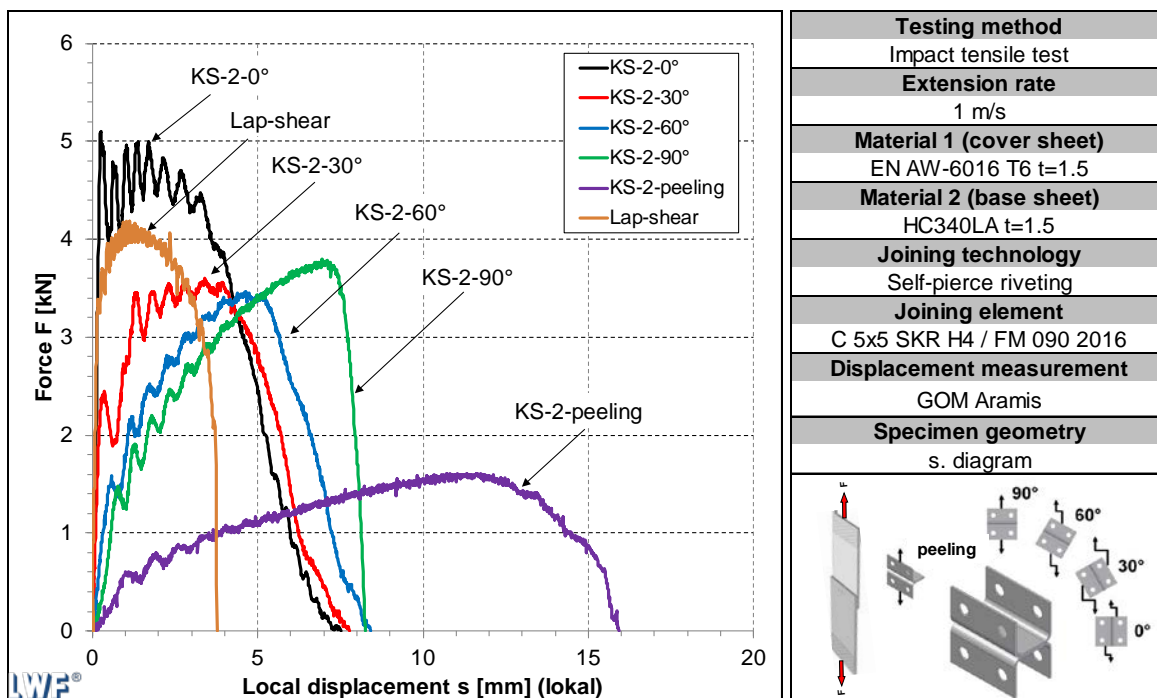


Figure 1: Characteristic force vs. displacement curves of the LWF-KS-2- and lap-shear tests for the SPR joint of EN AW-6016 T6(1.5 mm) and HC340LA(1.5 mm) under impact loading

The force vs. displacement curves and maximum load are significantly influenced by the initial angle of load application. The maximum load is about 4.8 kN at LWF-KS-2-0° loading, i.e. shear loading. At 30°- and 60°- loading the maximum load reduces to 3.5 kN and 3.4 kN, respectively. In accordance to the quasi-static test results the maximum load under LWF-KS-2-90° loading, i.e. head tension, again increases slightly to 3.8 kN. The lowest maximum loads are measured under coach peel loading. Also the maximum loads measured in the lap-shear tests are comparable between quasi-static and impact loading. Indeed, on an overall basis, the maximum loads measured under quasi-static and impact loads are nearly on the same level for each load case because of the small and negligible positive strain rate effect of the ultimate tensile strength of the aluminum sheet metal on punch side

Additional to the experimental investigations with LWF-KS-2 tests on a specimen level with one single joint, component tests with T-joint specimens are conducted to validate the prediction algorithms and the parameter determination of the *CONSTRAINED_INTERPOLATION_SPOTWELD (Model 2, "SPR4"). The T-joint specimen with the severe loaded joints and the schematic sketch of the test set up are shown in Figure 2 for

longitudinal and lateral loading direction. The component tests have been performed under quasi-static and impact loading velocities at the LWF.

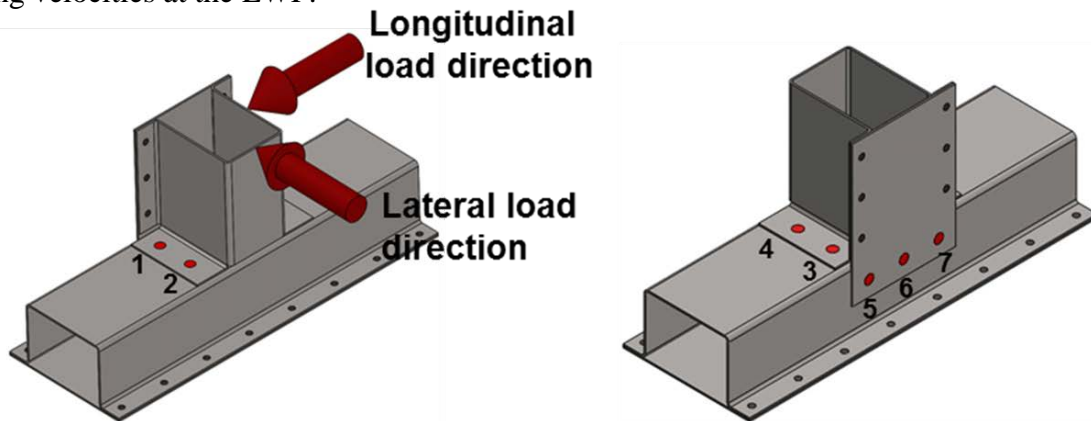


Figure 2: Geometry of T-joint specimen, loading directions for quasi-static and impact tests and numbering of rivets

The original and unfiltered force vs. displacement curves of the T-joint specimen tests are shown in Figure 3 for the lateral loading with a testing velocity of 1 m/s. The force signal is superimposed with oscillations because of the dynamic effects occurring during impact tests. A characteristic force vs. displacement curve (dashed line) measured under quasi-static loading is plotted additionally to the curves measured under impact loading. Generally, the same characteristics are observed concerning the failure sequence and failure points in time. The rivets 2 and 4 have failed through head pullout on the punch sided sheet metal of the joint after the maximum load of about 3.5 kN was reached. Afterwards the load signal has decreased steadily and reached a local minimum before it has risen again to a local load maximum. There, the rivets 1 and 3 have failed. Here again these rivets have failed through head pullout on the punch sided part of the component.

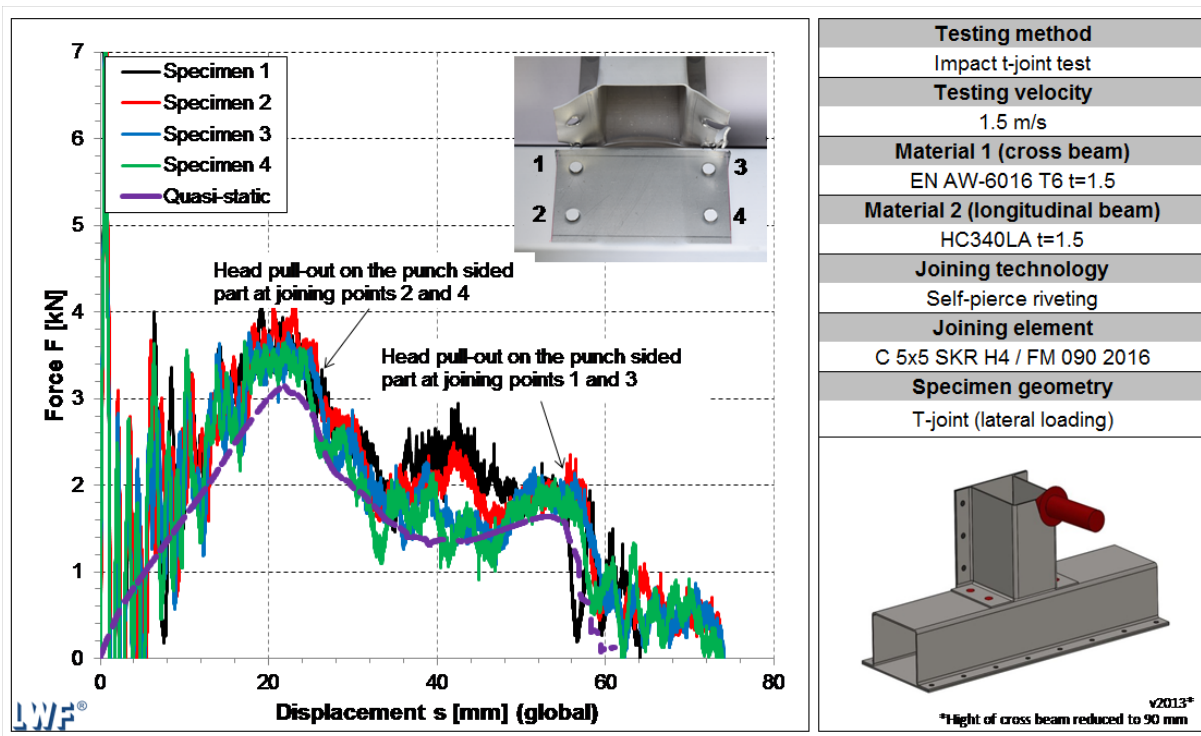


Figure 3: Test results of the T-joint specimens made of EN AW-6016 T6 (1.5 mm) and HC340LA (1.5 mm) and joined with SPR-ST joints at lateral impact loading

Constraint_SPR3 model and parameter determination

The *CONSTRAINED_INTERPOLATION_SPOTWELD (Model 2, "SPR4") is based on the calculation of the relative motions of the connected sheets. By definition of a reference node N_{ref} , which locates the position of the fastener, and a related radius r of the domain of influence the nodes of the connected sheets are determined, which are used to represent the connection. These nodes can be used to calculate the unit vectors \vec{n}_m and \vec{n}_s , which are orthogonal to the master and the slave sheet, respectively. By averaging the normal vectors of both sheets

$$\vec{n}_n = \frac{\vec{n}_m + \vec{n}_s}{|\vec{n}_m + \vec{n}_s|} \quad (1)$$

the direction of normal loads and by the equation

$$\vec{n}_t = (\vec{n}_s \times \vec{n}_m) \times \vec{n}_m \quad (2)$$

the shear direction can be identified. The total relative displacement $\vec{\delta}$ can be divided into two parts, one part δ_n in direction of \vec{n}_n

$$\delta_n = \vec{\delta} \cdot \vec{n}_n \quad (3)$$

and the second part δ_t in direction \vec{n}_t

$$\delta_t = \vec{\delta} \cdot \vec{n}_t. \quad (4)$$

This vector of the relative motion can be used to get the transferred forces and moments and to describe the flow and failure behavior and is calculated by

$$\vec{u} = [\delta_n, \delta_t]. \quad (5)$$

In addition sym , which is an indicator for the symmetry of the rivet load, is calculated by

$$sym = \arccos \frac{\vec{n}_s \cdot \vec{n}_m}{|\vec{n}_s| |\vec{n}_m|} \quad (6)$$

Considering the joint stiffness $STIFF$ the transferred forces can be determined by

$$\vec{f} = [f_n, f_t] = STIFF \cdot \vec{u} = STIFF \cdot [\delta_n, \delta_t]. \quad (7)$$

Associated plastic flow with the yield surface

$$\left[\left(\frac{f_n}{R_n \cdot (1 - \alpha_1 \cdot sym)} \right)^{\beta_1} + \left(\frac{f_s}{R_s} \right)^{\beta_1} \right]^{\frac{1}{\beta_1}} - F^0(\bar{u}^{pl}) = 0 \quad (8)$$

is implemented including the parameters R_n and R_s , the load capacities in normal and shear direction, a scale factor α_1 for reduction of normal load capacity in unsymmetrical loading cases i.e. bending, the exponent β_1 defining the mixed-mode behavior and the yield curve $F^0(\bar{u}^{pl})$ with the equivalent plastic displacement \bar{u}^{pl} . Linear scaling of the transferred forces

$$\vec{f}^* = (1 - d)\vec{f} \quad (9)$$

with the damage value

$$d = \frac{\bar{u}^{pl} - \bar{u}_0^{pl}}{\bar{u}_f^{pl} - \bar{u}_0^{pl}} \quad (10)$$

is done. For this purpose the equivalent plastic displacement at failure \bar{u}_f^{pl} and the equivalent plastic displacement at damage initiation \bar{u}_0^{pl} are calculated considering the load angle φ

$$\varphi = \arctan\left(\frac{f_n}{f_s}\right) \quad (11)$$

and the following equations for damage initiation and failure

$$\left[\left(\frac{\bar{u}_0^{pl,n}}{\bar{u}_{0,ref}^{pl,n} \cdot (1 - \alpha_2 * sym)} \right)^{\beta_2} + \left(\frac{\bar{u}_0^{pl,s}}{\bar{u}_{0,ref}^{pl,s}} \right)^{\beta_2} \right]^{\frac{1}{\beta_2}} - 1 = 0 \quad (12)$$

$$\bar{u}_0^{pl,n} = \sin(\varphi) \cdot \bar{u}_0^{pl} \quad (13)$$

$$\bar{u}_0^{pl,s} = \cos(\varphi) \cdot \bar{u}_0^{pl} \quad (14)$$

$$\left[\left(\frac{\bar{u}_f^{pl,n}}{\bar{u}_{f,ref}^{pl,n} \cdot (1 - \alpha_3 * sym)} \right)^{\beta_3} + \left(\frac{\bar{u}_f^{pl,s}}{\bar{u}_{f,ref}^{pl,s}} \right)^{\beta_3} \right]^{\frac{1}{\beta_3}} - 1 = 0 \quad (15)$$

$$\bar{u}_f^{pl,n} = \sin(\varphi) \cdot \bar{u}_f^{pl} \quad (16)$$

$$\bar{u}_f^{pl,s} = \cos(\varphi) \cdot \bar{u}_f^{pl}. \quad (17)$$

with the parameters equivalent plastic displacement at damage initiation in normal and shear direction $\bar{u}_{0,ref}^{pl,n}$ and $\bar{u}_{0,ref}^{pl,s}$, respectively; the equivalent plastic displacement at failure in normal and shear direction $\bar{u}_{f,ref}^{pl,n}$ and $\bar{u}_{f,ref}^{pl,s}$, respectively. Furthermore the parameters α_2 and α_3 for reduction of equivalent plastic displacement at damage initiation and the equivalent plastic displacement at failure in normal direction in unsymmetrical loading cases i.e. bending, $\bar{u}_{0,ref}^{pl,n}$ and $\bar{u}_{f,ref}^{pl,n}$, respectively. The exponents, β_2 and β_3 , are defining the mixed-mode behavior of the equivalent plastic displacement at damage initiation and failure, respectively.

The parameter identification can be done in the following seven steps including reverse engineering i.e. simulation of the experiments and fitting some of the parameters to the experimental measured force vs. displacement curves. At least force vs. displacement curves for shear loading, tensile loading, one mixed mode loading i.e. 30° or 45° or 60° and peel loading should be available. If in the following chapter “Validation” is spoken about “manually determined parameter set” this seven step procedure is supposed.

Step 1: *Domain of influence*

In the first step the radius of the domain of influence must be defined. This value should be equal or in the order of the rivet head diameter for shell elements with edge length greater 2.5 mm, not the rivet head radius as possibly assumed.

Step 2: *Stiffness*

The stiffness $STIFF$ of the joint can be determined by the force vs. displacement curve of a shear test of the joint like LWF-KS-2-0° or a lap shear test with small sheet deformation. Based on the small deformations of the sheets $STIFF$ can be estimated in the linear area by

$$STIFF = \frac{\Delta F}{\Delta s} \quad (18)$$

Thereby ΔF and Δs are the force and displacement differences in the approximately linear area of the force vs. displacement curve, in which the stiffness will be averaged.

Step 3: *Shape of the flow curve*

Also the flow curve can be determined using the results of shear specimen tests. As for the determination of the stiffness, the approach is based on the assumption that the deformations of the sheets are very small and only local deformations occur. These small and local deformations cannot be described by discretization usually used in crash simulation. So these are all included in the plastic deformations of the simplified model.

$$u_{pl} = \left(s - \frac{F(s)}{STIFF} \right) R_s \quad (19)$$

Step 4: *Maximum Forces*

The maximum transferred forces by the *CONSTRAINED_INTERPOLATION_SPOTWELD (Model 2, "SPR4") represented by the parameters R_n and R_s are equal to the maximum measured forces in case of a normal and shear specimen test, respectively.

Step 5: *Combination of shear and tensile load*

The behavior in case of combined shear and tensile load is determined using LWF-KS-2-30° or -60° test results. Also it is possible to use another test with a combined shear and tensile load. Solving the equation

$$\left(\frac{f_n}{R_n} \right)^{\beta_1} + \left(\frac{f_s}{R_s} \right)^{\beta_1} = 1 \quad (20)$$

with the maximum force split in the normal and shear fraction by

$$f_n = \sin\varphi \cdot F_{max}^\varphi \quad (21)$$

$$f_s = \cos\varphi \cdot F_{max}^\varphi \quad (22)$$

leads to the value of β_1 .

Step 6: *Damage and Failure behavior*

The determination of the parameters for the damage initiation and failure behavior $\bar{u}_{0,ref}^{pl,n}$, $\bar{u}_{0,ref}^{pl,s}$, $\bar{u}_{f,ref}^{pl,n}$ and $\bar{u}_{f,ref}^{pl,s}$ are be done by reverse engineering.

Step 7: *Influence of sym*

Also the weighting coefficients $\alpha_1, \alpha_2, \alpha_3$ should be determined by reverse engineering using peeling test results.

Transformation rules have been developed for an automatically determination and calculation of parameters out of test results. Some simplifications have to be assumed and still some parameters are only determinable with empirical approaches.

The equivalent plastic displacement \bar{u}^{pl} is defined with the energy equivalent

$$\int F_{ref} d\bar{u}^{pl} = \int \sum_i f_i du_i^{pl} \quad (23)$$

and the transformation rule for \bar{u}^{pl} out of measured displacement u_{exp}^{pl} is given to

$$\bar{u}^{pl} = W_{exp}^{pl} = \int f_{exp} du_{exp}^{pl} \quad (24)$$

with the assumptions

$$F_{ref} = F^0(\bar{u}^{pl}) = 1 \quad (25)$$

and

$$\int \sum_i f_i du_i^{pl} = W_{exp}^{pl} \quad (26)$$

i.e. the dissipated plastic work is equal in simulation and experiment. The scaling of the measured experimental force curve f_{exp} of a LWF-KS-2-0° test could be done with the simplified assumption that $f_n = 0$ and $f_s = f_{exp}$ in this experiment. Of course there will be a slightly rotation of the rivet until reaching maximum force f_{max} even in the quite stiff LWF-KS-2-0° specimen, but this is neglected in this simplified assumption. Simultaneously an analytical exponential equation is chosen for the yield curve

$$F^0(\bar{u}^{pl}) = \begin{cases} a(b - \bar{u}^{pl})^c + d & \text{for } \bar{u}^{pl} < b \\ 1 & \text{for } \bar{u}^{pl} \geq b \end{cases} \quad (27)$$

with $d = 1$, $b = \bar{u}_{fmax}^{pl}$, $a = \frac{k-1}{b^c}$ and $k = \frac{f_{yield}}{f_{max}}$ with force at the onset of beginning of plastic deformation f_{yield} and the maximum force f_{max} and exponent $c > 0$, a fitting parameter. In Figure 4 an example for the transformation rule and fitting of $F^0(\bar{u}^{pl})$ is shown.

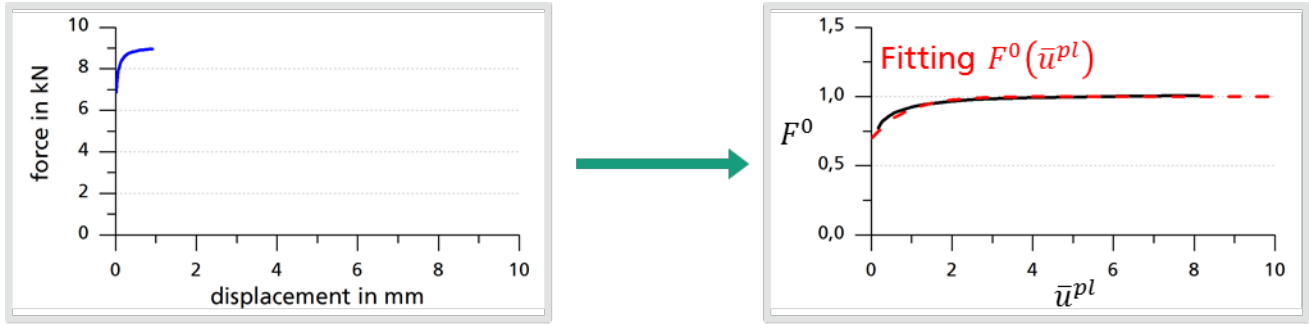


Figure 4: Force vs. displacement cure of a LWF-KS-2-0° shear test until force maximum (left) and normalized yield curve $F^0(\bar{u}^{pl})$ (right) obtained by fitting the analytical exponential equation (27)

The equivalent plastic displacement at damage initiation \bar{u}_0^{pl} and the equivalent plastic displacement at failure \bar{u}_f^{pl} can also be calculated on the basis of the definition of the equivalent plastic displacement (23), (25) and (26) and the yield function $F^0(\bar{u}^{pl})$ fitted to (27) and by integration and dissolving. So the equivalent plastic displacement at damage initiation is given by

$$\bar{u}_0^{pl} = W_{exp,f} - W_{exp,f}^{el} - W_{exp,f}^{sheet} - \bar{u}_{fmax}^{pl} \left(\frac{k-1}{c+1} \right) \quad (28)$$

and equivalent plastic displacement at failure by

$$\bar{u}_f^{pl} = 2(W_{exp,f} - W_{exp,f}^{sheet}) - W_{exp,0} + W_{exp,0}^{el} + W_{exp,0}^{sheet} - \bar{u}_{fmax}^{pl} \left(\frac{k-1}{c+1} \right) \quad (29)$$

with the total work until failure $W_{exp,f}$, i.e. the complete surface under the experimental force vs. displacement curve

$$W_{exp,f} = W_{exp,f}^{pl} + W_{exp,f}^{el} + W_{exp,f}^{sheet} \quad (30)$$

which is a sum of plastic work $W_{exp,f}^{pl}$ and elastic work $W_{exp,f}^{el}$ performed on the joint and the performed work of the sheet $W_{exp,f}^{sheet}$, i.e. the total deformation energy of the jointed sheet metals. $W_{exp,0}$ is the total work performed until damage initiation is reached, i.e. the surface under the experimental force vs. displacement curve until damage initiation displacement $u_{exp,0}$ is reached (see hatched area in Figure 5)

$$W_{exp,0} = W_{exp,0}^{pl} + W_{exp,0}^{el} + W_{exp,0}^{sheet} \quad (31)$$

which is a sum of the plastic work $W_{exp,0}^{pl}$ and elastic work $W_{exp,0}^{el}$ performed on the joint and the performed work of the sheet $W_{exp,0}^{sheet}$ until damage initiation is reached.

The calculation of the parameters for the damage initiation and failure behavior $\bar{u}_{0,ref}^{pl,n}$, $\bar{u}_{0,ref}^{pl,s}$, $\bar{u}_{f,ref}^{pl,n}$ and $\bar{u}_{f,ref}^{pl,s}$ of *CONSTRAINED_INTERPOLATION_SPOTWELD (Model 2, "SPR4") can be done by executing equation (28) and (29) with a force vs. displacement curve $f_{exp}^{90^\circ}(u_{exp})$ of a LWF-KS-2-90° test for the parameters $\bar{u}_{0,ref}^{pl,n}$ and $\bar{u}_{f,ref}^{pl,n}$ for normal direction and $f_{exp}^{0^\circ}(u_{exp})$ of a LWF-KS-2-0° test for the parameters $\bar{u}_{0,ref}^{pl,s}$ and $\bar{u}_{f,ref}^{pl,s}$ for shear direction. β_2 and β_3 are determined according to β_1 with \bar{u}_0^{pl} and \bar{u}_f^{pl} of a mixed-mode loading like the LWF-KS-2-30°-test and equations (12) to (17).

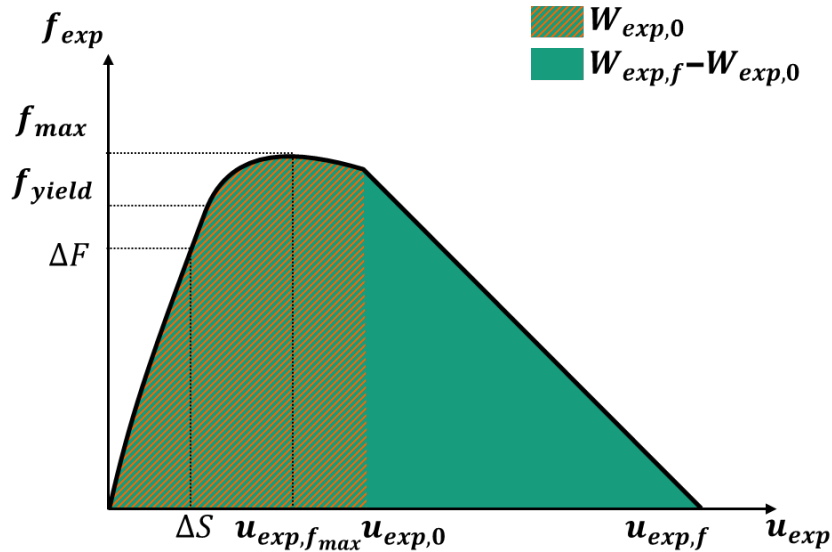


Figure 5: Schematic sketch of an experimental measured force vs. displacement curve $f_{exp}(u_{exp})$ with selected parameters

But there are still some parameters left, which are not directly calculable, namely the parameters or weighting coefficients $\alpha_1, \alpha_2, \alpha_3$ for bending, see equations (8), (12) and (15). Also the deformation energies of the sheets, $W_{exp,0}^{sheet}$ and $W_{exp,f}^{sheet}$, are not directly calculable without the results of a LS-DYNA simulations of LWF-KS-2 tests.

A lot of testing and simulation results are available for SPR-ST joints for different sheet materials and sheet thicknesses at Fraunhofer IWM. On this database an empirical approach for $\alpha_1, \alpha_2, \alpha_3, W_{exp,0}^{sheet}$ and $W_{exp,f}^{sheet}$ was developed in dependence of ultimate tensile strengths and thicknesses of the joined sheets and fit parameters. This approach is implemented in JoingLab for SPR-ST joints only. For all other joining technique the parameters $\alpha_1, \alpha_2, \alpha_3, W_{exp,0}^{sheet}$ and $W_{exp,f}^{sheet}$ are set to zero by JoingLab.

Prediction algorithms for mechanical properties

The aim of the prediction of mechanical properties, i.e. some of the characteristic points in the force vs. displacement curve, is the generation of model parameters for crash simulation of unknown, untested joints. Therefore a procedure in the range of multivariate regression has been developed and implemented in [1]. The basis for the forecast is a dataset for training, i.e. an amount of connections and their mechanical parameters, on which the prediction algorithm adapts its underlying models. The procedures require input and output parameters for the calibration and prediction functionalities. The input parameters are describing the connected materials and the connection itself. Output parameters are the properties, which can be determined by experimental testing. The properties, which have to be predicted, are subdivided in two categories. The properties of the first category are directly readable and calculable out of the measured force vs. displacement curve, e.g. maximum load, load at damage initiation, work until maximum load, work until damage initiation and work until failure. The properties of the second category need algorithms to be determined, e.g. stiffness of the joint, onset of yielding and hardening behavior. Procedures have been developed to automatically determine the parameters of the properties of the second category for all supported joining techniques. Model parameters of the *CONSTRAINED_INTERPOLATION_SPOTWELD (Model 2, “SPR4”) are automatically derived out of the properties by means of translation rules developed by the Fraunhofer IWM and described in the previous chapter. The forecast of properties for an unknown connection is carried out in two steps. In the first step, the corresponding properties are determined for all available connection data of the dataset for training. The forecast algorithms are calibrated in a learning method together with the material and connection specific parameters. In the second step the properties of the unknown connection (output parameters) are predicted on basis of the calibrated forecast algorithms and the connection parameters of the unknown joint (input parameters) selected by the user. The joint tested for validation purposes is a self-piercing riveted connection of aluminum EN AW-6016 with sheet thickness of 1.5 mm and steel HC340LA with 1.5 mm sheet thickness. Of course this validation connection is not part of the dataset for training. Figure 6 shows the relative deviation between the predicted properties of the forecast algorithm and the automatically derived properties out of the force vs. displacement curves of the tested validation connection. The underlying dataset of training contains three tested and well known joints.

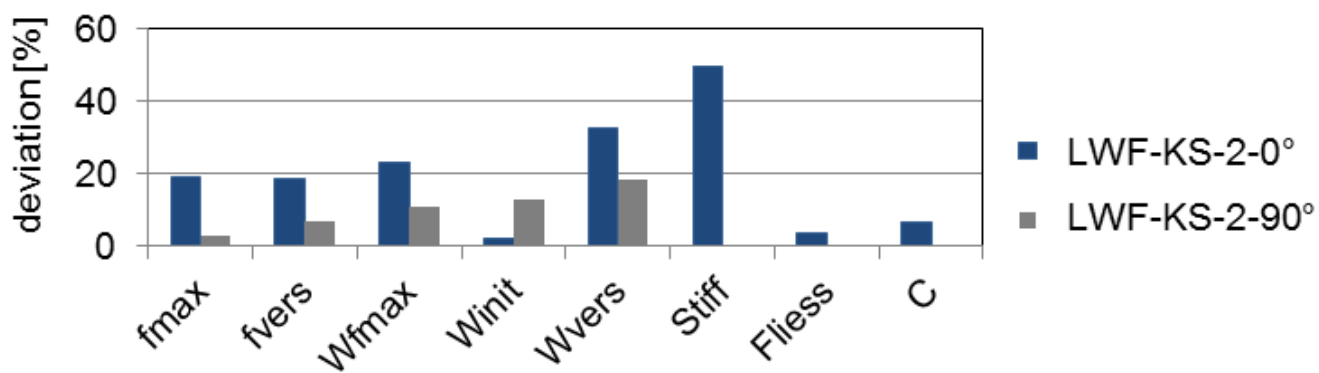


Figure 6: Relative deviations of the predicted properties of the validation joint for LWF-KS-2-0° and -90° tests

All developed algorithms are implemented in the software JoiningLab. Additionally, JoiningLab provides the capability to store, to manage, to visualize and to assess the joint properties of tested mechanical joints of different joining techniques on the base of well-defined parameters (see Figure 7). Furthermore, the software contains algorithms to search and show similar joints dependent on user defined input parameters. Also the encryption of datasets is possible. A database management system (Oracle or Microsoft Access) is integrated in JoiningLab for an enhancement of the maintainability and a higher efficiency and quality of the data management.

Furthermore a function for automatization of the forecast settings and forecast execution is provided for the developed multivariate regression algorithms.



Figure 7: main window (overview over all connections) of the software JoiningLab

Validation

The validation of the automatically determined and the predicted model parameters of the *CONSTRAINED_INTERPOLATION_SPOTWELD (Model 2, “SPR4”) model was done based on experimental results for a connection between an aluminum sheet (EN AW 6016 in $t=1.5$ mm) and a steel sheet (HC340LA in $t=1.5$ mm) joined with SPR, punch-riveting, FDS and tac-setting tested with the LWF-KS-2 test assembly and a T-joint specimen. The LWF-KS-2-Specimens were simulated with the automatically determined and the predicted model parameters and with a manually determined parameter set. The same parameter sets were used to simulate the component tests with the T-joint specimens as well.

Figure 8, Figure 9 and Figure 10 show the force vs. displacement curves of the tested and the simulated LWF-KS-2-specimens of the joint EN AW-6016, $t=1.5$ mm in HC340LA, $t=1.5$ mm joined with SPR-ST. The FE-model of the LWF-KS-2-specimens is illustrated in Figure 10 right side for the different load cases. There is a good match between experiment and simulation regarding the load bearing capacity under the different load cases for all model parameter sets. Only the simulated results of the peeling specimen show an overestimated maximum force for automatically determined and predicted model parameters. This is because the parameters for bending behavior are not considered in these two models. The simulation with predicted model parameters shows slightly overestimated load bearing capacities under combined loading (LWF-KS-2-60° and -30°). The stiffness is fitted on the basis of the KS-0°-specimen, the load case with the least sheet metal deformation. Because the *CONSTRAINED_INTERPOLATION_SPOTWELD (Model 2, “SPR4”) does not allow a calibration of the stiffness independent of the load direction the linear elastic area of the force vs. displacement

curves deviates from the experimental results with an increasing load angle. The displacement of the onset of yielding is predicted well by the models with manually and automatically determined parameters. Only under normal load (LWF-KS-2-90°) there is an underestimation observable which is due to the low stiffness. The simulation results with predicted model parameters show displacement of the onset of yielding and displacement of failure which are too small for all load cases. The simulation results with automatically determined parameters overestimate the displacement at failure under LWF-KS-2-0°, LWF-KS-2-30° and LWF-KS-2-60° loading angles. For LWF-KS-2-90° and peeling load there is an underestimation of the displacement at failure observable. With manually determined model parameters the displacement at failure matches well with the experimental data for the LWF-KS-2-0°, LWF-KS-2-90° and peeling tests. In the case of LWF-KS-2-30° loading, there is a slight underestimation noticeable in contrast to LWF-KS-2-60°, where the displacement at failure is overestimated.

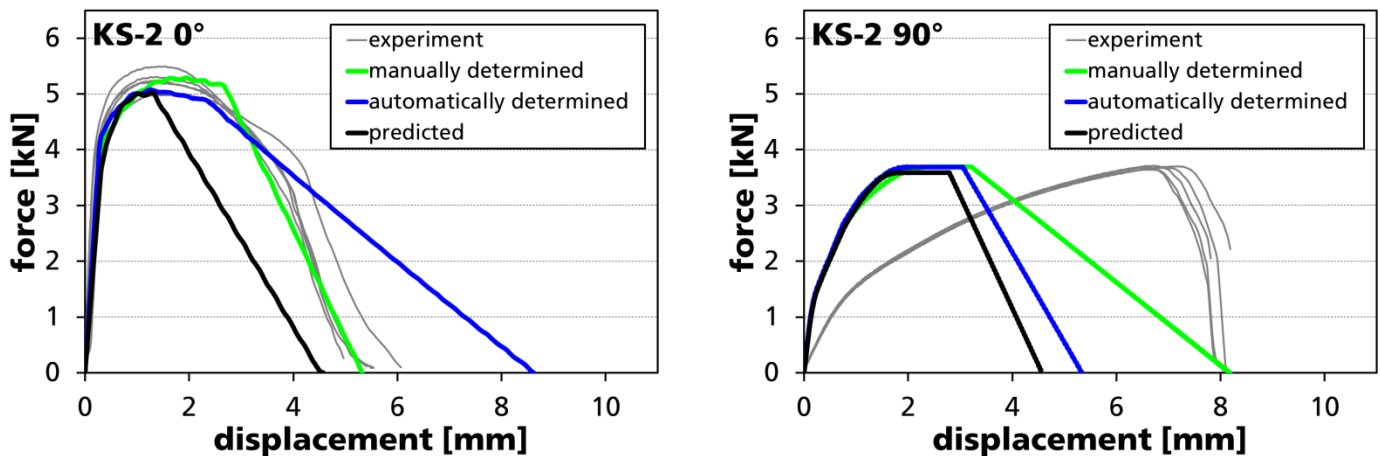


Figure 8: Force vs. displacement curves of the quasi-static tested and the simulated LWF-KS-2-specimens of the SPR-ST joint EN AW-6016, t=1.5mm in HC340LA, t=1.5mm: *CONSTRAINED_SPR3 (Model 2, “SPR4”), left: LWF-KS-2-0° load; right: LWF-KS-2-90° load

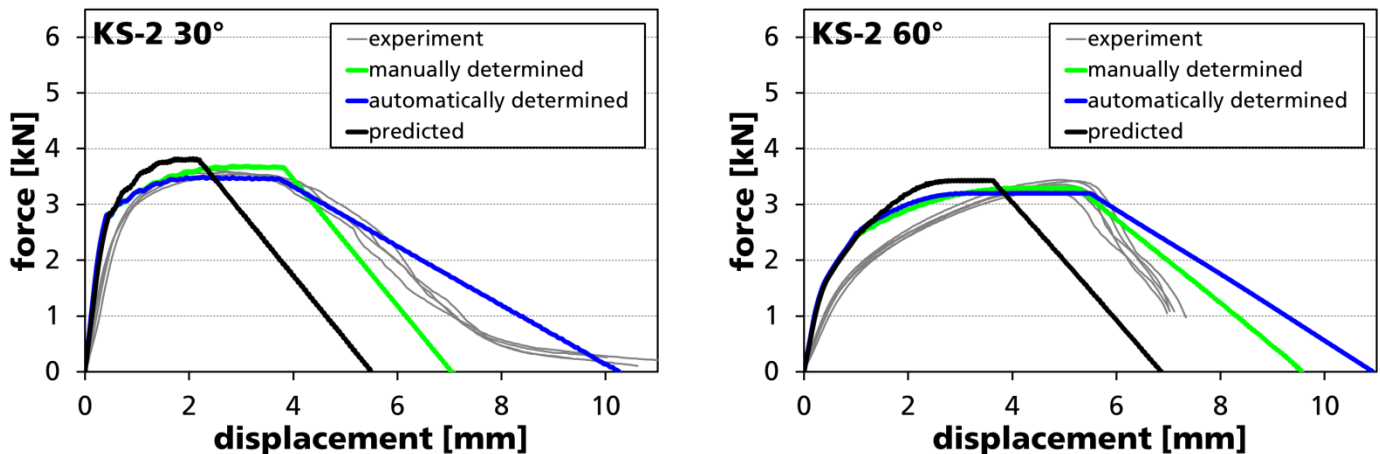


Figure 9: Force vs. displacement curves of the quasi-static tested and the simulated LWF-KS-2-specimens of the SPR-ST joint EN AW-6016, t=1.5mm in HC340LA, t=1.5mm: *CONSTRAINED_SPR3 (Model 2, “SPR4”), left: LWF-KS-2-30° load direction; right: LWF-KS-2-60° load direction

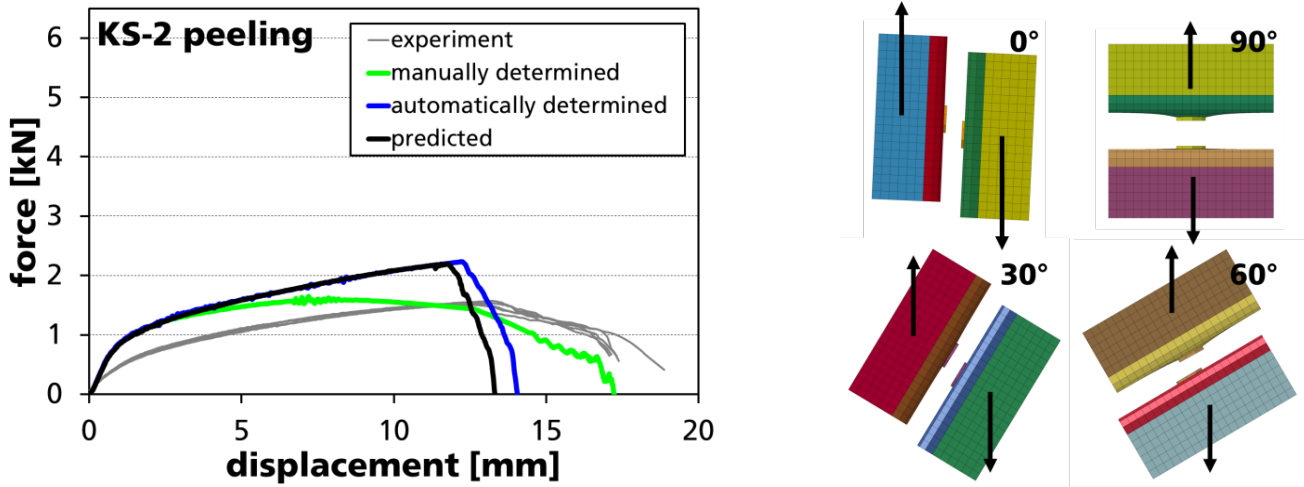


Figure 10: Force vs. displacement curves of the quasi-static tested and the simulated LWF-KS-2-specimens of the SPR-ST joint EN AW-6016, $t=1.5\text{mm}$ in HC340LA, $t=1.5\text{mm}$:*CONSTRAINED_SPR3 (Model 2, "SPR4"), left: LWF-KS-2 peel loading; right: FE-models of LWF-KS-2 specimen

The Figure 11 shows the experimental and simulation results of the component test with the T-joint specimen under quasi-static and lateral loading. There is a good correlation between the load bearing capacities of the simulation results with automatically determined and predicted model parameters and the experimental results. The simulation result with manually determined parameters slightly underestimates the force at failure of the rivets 2 and 4 as well as of the rivets 1 and 3. At failure of the rivets 2 and 4 the displacement is slightly larger than in the experiment for automatically and manually determined model parameters. The force vs. displacement curve at the time of failure of the rivets 1 and 3 shows an overestimation of the displacement for all model parameter sets. All in all there is a correlation between the failure behavior of the rivets of the T-joint specimens and the behavior of the model under LWF-KS-2-peeling load. The relation between the force vs. displacement curves of the LWF-KS-2 peeling specimen corresponds with the results of the T-joint simulation. This is caused by the similar loading conditions at the relevant rivets.

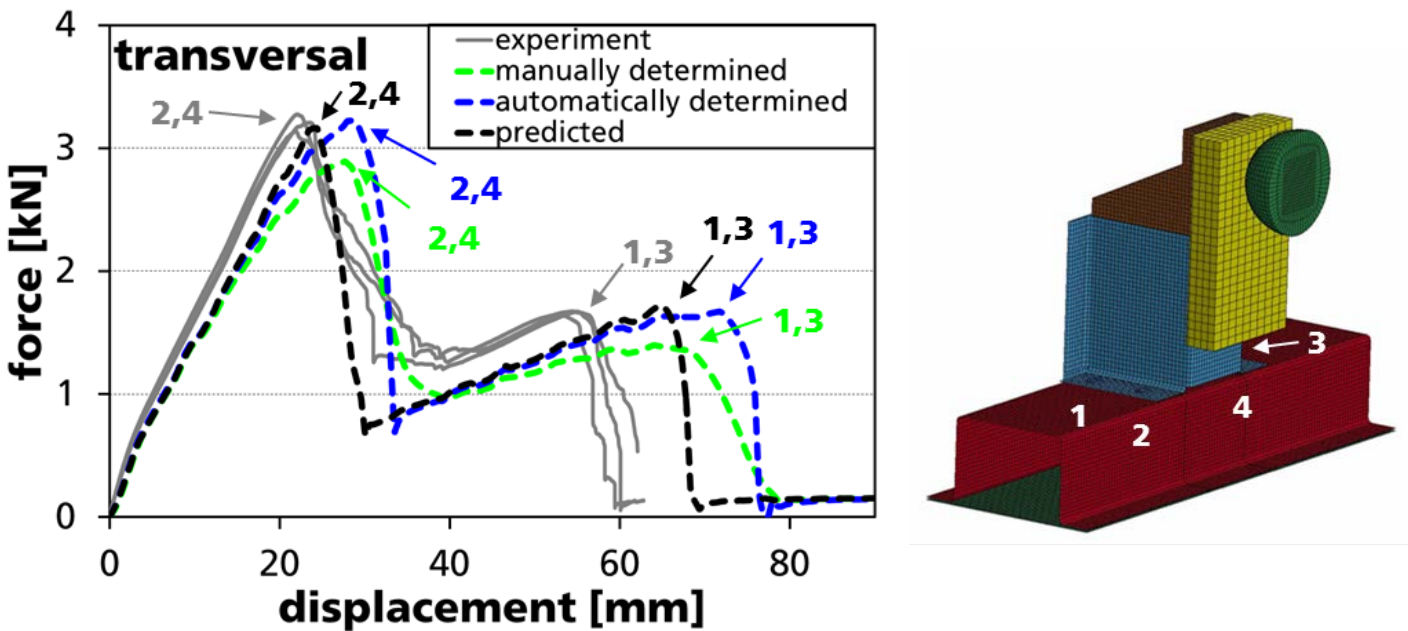


Figure 11: Force vs. displacement curves and failure points of rivets of the tested and simulated T-joint specimens under quasi-static lateral loading (left) and numbering of rivets (right)

The force vs. displacement curves of the experiment and the simulation of the T-joint specimens for the joint EN AW-6016, $t=1.5\text{mm}$ in HC340LA, $t=1.5\text{mm}$ joined with SPR under quasi-static longitudinal load are illustrated in Figure 12. The simulations with manually and automatically determined parameters show a good correlation with the experimental data. The force level at failure of the rivets 5, 3, 4 and 6 matches well with the test results. In comparison to the experiment the failure of rivet 7 occurs much later. This is because the *CONSTRAINED_INTERPOLATION_SPOTWELD (Model 2, “SPR4”) cannot transfer any torsional moments. Moreover there is a deviation in the shape of the force vs. displacement curves of the simulation with automatically determined parameters and the experiments at failure of the rivet 5. Because the displacement at failure of the LWF-KS-2-0° specimen is overestimated the T-joint model cannot describe the reduction in force during failure of the rivet 5 correctly. The failure behavior of the T-joint under longitudinal load is mainly dominated by the model parameters which adjust shear loading. That is why the relations between the force vs. displacement curves of the T-joint simulations with the different model parameter sets correspond to the ones of the LWF-KS-2-0° specimen simulations. In accordance to the results of LWF-KS-2-0° simulation the component simulation with predicted model parameters shows an underestimated maximum force at failure of rivet 5. Due to the small displacement at failure under shear loading (LWF-KS-2-0°) the failure of the rivet 7 occurs too early in the component simulation.

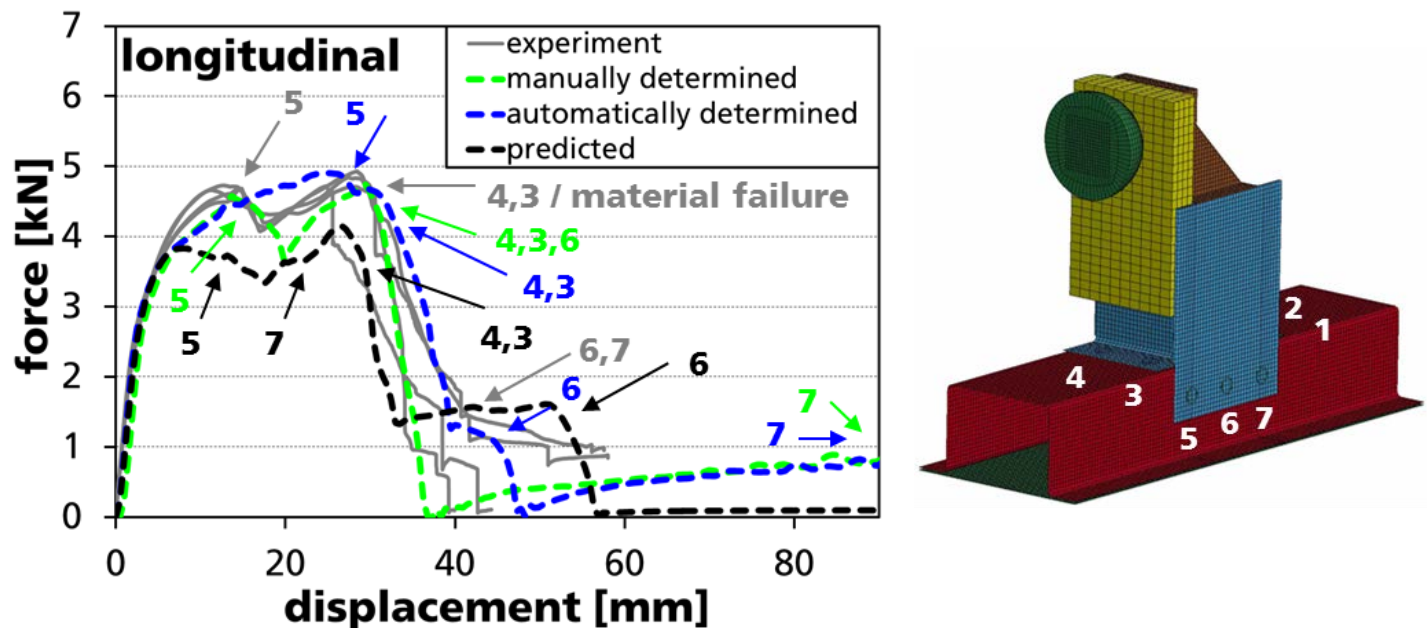


Figure 12: Force vs. displacement curves and failure points of rivets of the tested and simulated T-joint specimens under quasi-static longitudinal loading (left) and numbering of rivets (right)

Summary

In this paper the software Joininglab was introduced, which was developed during the public German AiF-project “CrasiFue” [1]. JoiningLab predicts the mechanical properties (characteristic points of the force vs. displacement curves) and finally generates the parameters of the *CONSTRAINED_INTERPOLATION_SPOTWELD (Model 2, “SPR4”) for crash simulation with LS-DYNA of untested, unknown mechanical joints. The required input parameters are the results of the experimental characterization of the joined materials and the joints. The shown test and simulation results have shown the successful application of the prediction software. Overall a good correlation of experimental measured force vs. displacement curves and on the basis of predicted properties, i.e. predicted model parameters, simulated force vs. displacement curves was achieved.

This applies on both, the tests with LWF-KS-2 specimens and the component tests with T-joint specimens. The software JoiningLab provides the user diverse possibilities for choosing, visualization, changing and assessment of databases for mechanical joints.

Acknowledgement

The IGF research project 18468 BG by research association Gesellschaft zur Förderung angewandter Informatik e. V. (GFaI), Berlin in cooperation with the Research Association for Steel Application. (FOSTA) and the Research Association for Automotive Technology (FAT), has been funded by the AiF under the program for promotion of industrial research (IGF) by the Federal Ministry of Economics and Energy based on a decision of the German Bundestag.

References

- [1] Herfert, D.; Guenther, M.; Hein, D.; Giese, P.; Rochel, P.; Sommer, S.: final report of IGF project “CraSiFue” 18468 BG, 2017.
- [2] Bier, M., Sommer, S.: “Simplified modeling of self-piercing riveted joints for crash simulation with a modified version of *CONSTRAINED_INTERPOLATION_SPOTWELD”, 9th European LS-DYNA Conference, Manchester, UK, 2013.
- [3] Bier, M., Sommer, S.: “Modeling of self-piercing riveted joints for crash simulation – state of the art and future topics”, 10th European LS-DYNA Conference, Wuerzburg, Germany, 2015.